Targeting glycolysis in endothelial cells to prevent intraplaque neovascularization and atherogenesis in mice

Perrotta, P.

Chapter 4

Partial inhibition of glycolysis reduces atherogenesis independent of intraplaque neovascularization in mice

Perrotta P*, Van der Veken B*, Van Der Veken P, Pintelon I, Roosens L, Adriaenssens E, Timmerman V, Guns PJ, De Meyer GRY, Martinet W.

Arterioscler Thromb Vasc Biol. 2020; 40:1168-1181

*The first two authors contributed equally to this work

Abstract

Objective: Intraplaque (IP) neovascularization is an important feature of unstable human atherosclerotic plaques. However, its impact on plaque formation and stability is poorly studied. Because proliferating endothelial cells (ECs) generate up to 85% of their ATP from glycolysis, we investigated whether pharmacological inhibition of glycolytic flux by the small molecule 3PO [3-(3-pyridinyl)-1-(4-pyridinyl)-2-propen-1-one] could have beneficial effects on plaque formation and composition.
Approach and results: ApoE$^{-/-}$ mice treated with 3PO (50 µg/g, i.p.; 4x/week, 4 weeks) showed a metabolic switch toward ketone body formation. Treatment of ApoE$^{-/-}$Fbn1$^{C1039G+/-}$ mice with 3PO (50 µg/g, i.p.) either after 4 weeks of western diet (WD) (preventive, twice/week, 10 weeks) or 16 weeks of WD (curative, 4x/week, 4 weeks) inhibited IP neovascularization by 50% and 38%, respectively. Plaque formation was significantly reduced in all 3PO-treated animals. This effect was independent of IP neovascularisation. In vitro experiments showed that 3PO favors an anti-inflammatory M2 macrophage subtype and suppresses an M1 pro-inflammatory phenotype. Moreover, 3PO induced autophagy, which in turn impaired NF-κB signalling and inhibited TNF-α-mediated VCAM-1 and ICAM-1 up-regulation. Consistently, a preventive 3PO regimen reduced endothelial VCAM-1 expression in vivo. Furthermore, 3PO improved cardiac function in ApoE$^{-/-}$Fbn1$^{C1039G+/-}$ mice after 10 weeks of treatment.
Conclusions: Partial inhibition of glycolysis restrained IP angiogenesis without affecting plaque composition. However, less plaques were formed, which was accompanied by downregulation of endothelial adhesion molecules, an event that depends on autophagy induction. Inhibition of coronary plaque formation by 3PO resulted in an overall improved cardiac function.

Keywords: atherosclerosis, intraplaque neovascularization, angiogenesis, glycolysis, 3PO

Graphical abstract

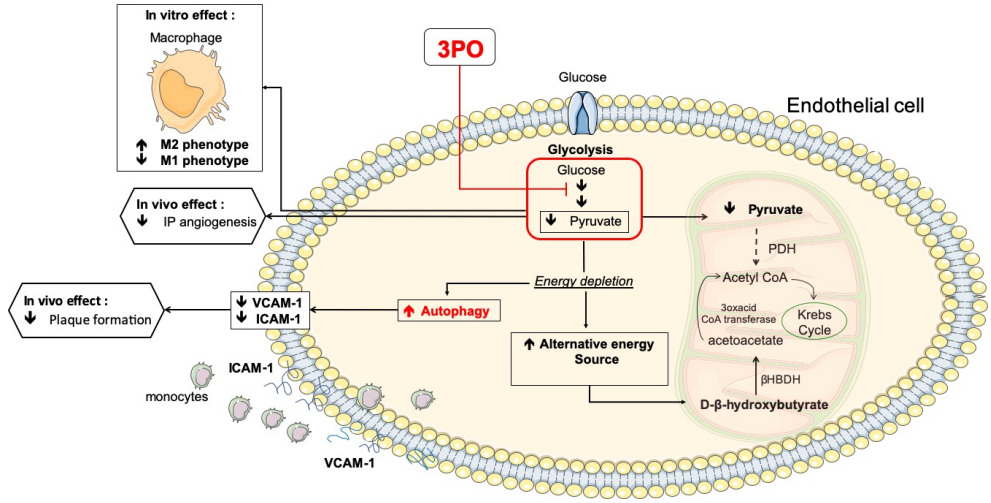

Highlights

- By using a mouse model of advanced atherosclerosis that develops IP neovascularization (ApoE$^{-/-}$Fbn1$^{C1039G+/-}$ mice) we found that partial inhibition of glycolysis impairs neovascularization in plaques
- Partial inhibition of glycolysis restrains atherosclerotic plaque formation independent of IP neovascularization and without affecting plaque composition
- Partial inhibition of glycolysis has a positive impact on cardiac function when administered in a preventive manner
- Partial inhibition of glycolysis increases the number of autophagosomes in endothelial cells
- Partial inhibition of glycolysis reduces endothelial VCAM-1 and ICAM-1 expression in an autophagy-dependent way
- Partial inhibition of glycolysis favors an anti-inflammatory M2 macrophage subtype and suppresses an M1 pro-inflammatory phenotype in vitro.

Introduction

Blood vessels constitute the largest network in our body to ensure a continuous blood flow towards different organs and tissues. However, despite their role in supplying nutrients and oxygenated blood, new vessels that branch off from existing vessels (a process known as neovascularization) could also play a detrimental role in various ischemic and inflammatory diseases including atherosclerosis.[1] Because intraplaque (IP) microvessels are immature and leaky,[2] they facilitate infiltration of lipids, inflammatory mediators and erythrocytes. Consequently, IP neovascularization has been linked to plaque progression.[3, 4] IP neovascularization is initiated in advanced plaques by hypoxia and emerges when the size or inflammatory burden of the plaque exceeds a critical threshold. Clinical trials targeting neovascularization in pathological settings mainly focus on blocking vascular endothelial growth factor (VEGF) signalling.[5] However, these studies have reported moderate success due to drug resistance or adverse effects.[6] Recent evidence indicates that proliferating endothelial cells (ECs) generate up to 85% of their ATP from glycolysis,[7] suggesting that EC metabolism is an attractive alternative target to reduce neovascularization.[8] Pharmacological inhibition of glycolytic flux by intra-peritoneal injection of the small molecule 3PO [3-(3-pyridinyl)-1-(4-pyridinyl)-2-propen-1-one] reduces vessel sprouting in EC spheroids, zebrafish embryos, mouse retina and models of inflammation.[9] 3PO dose dependently reduces glycolysis in ECs, but by no more than 35-40%, thus less than the nonmetabolizable glucose analog 2-deoxy-D-glucose, which reduces glycolysis by approximately 80%.[9] Because 3PO reduces cellular fructose-2,6-bisphosphate levels, it has been proposed that 3PO targets 6-phosphofructo-2-kinase/fructose-2,6-bisphosphatase 3 (PFKFB3).[10]However, more recent findings indicate that 3PO does not bind PFKFB3 and may act through mechanisms that are unrelated to PFKFB3inhibition.[11] Importantly, suppression of glycolysis by 3PO occurs without lowering the energy charge or increasing oxygen consumption, and without abrogating side metabolic pathways such as the pentose phosphate pathway necessary for NADPH production. Although inhibition of glycolysis by 3PO is partial and transient, it is sufficient to reduce neovascularization.[9]

IP neovascularization is a typical feature of advanced human atherosclerotic plaques, but is rarely observed in animal models.[12] Nonetheless, our group has recently reported that apolipoprotein E deficient ($ApoE^{-/-}$) mice, containing a heterozygous mutation (C1039G+/-) in the fibrillin-1 (Fbn1) gene, display substantial IP neovascularization in the brachiocephalic artery and common carotid arteries.[13] Because Fbn1 is the major structural component of extracellular microfibrils in the vessel wall, neovascularization in $ApoE^{-/-}Fbn1^{C1039G+/-}$ mice probably occurs because elastin fragmentation allows microvessel sprouting from the adventitial vasa vasorum through the media into the intimal lesion.[14] Moreover, the high degree of stenosis and presence of activated macrophages in plaques of $ApoE^{-/-}Fbn1^{C1039G+/-}$ mice likely results in IP hypoxia, and triggers the growth of new vessels from the adventitia.[14, 15] In the present study, we explored the possibility of inhibiting IP angiogenesis with 3PO in $ApoE^{-/-}Fbn1^{C1039G+/-}$ mice and studied its potential plaque stabilizing effects.

Material and methods

The authors declare that all supporting data are available within the article (and its online supplementary files).

Mice

Female $ApoE^{-/-}$ mice were fed a western-type diet (WD) (Altromin, C1000 diet supplemented with 20% milkfat and 0.15% cholesterol, #100171), starting at the age of 8 weeks, and treated with glycolysis inhibitor 3PO (50 mg/kg, i.p., 4x/week) or vehicle (DMSO) for 4 weeks. The animals were housed in a temperature-controlled room with a 12-hour light/dark cycle and had free access to water and food [either normal laboratory diet (ssniff, R/M-H) or WD]. To perform a glucose tolerance test, mice were fasted for 16 hours and injected with glucose (1 g/kg, i.p.). Blood glucose levels were determined and plotted in function of time. Insulin action was evaluated in vivo by injection of insulin (Novorapid, 1 U/kg, i.p.). Food and water intake of mice that were individually housed in metabolic cages (Tecniplast, floor area: 200 cm^2) were monitored for 24 hours. Mice in metabolic cages were weighted at the start of

the experiment and after 24 hours in the cage. Fasting and non-fasting blood glucose levels were analyzed with a hand-held glucometer (OneTouch Ultra, range 20-600 mg/dL; Lifescan) by taking a droplet of blood from the tip of the mouse's tail. At the end of the experiment, blood samples were obtained from the retro-orbital plexus of anesthetised mice (sodium pentobarbital 75 mg/kg, i.p.). Subsequently, mice were sacrificed with sodium pentobarbital (250 mg/kg, i.p.). Plasma samples were analyzed with an automated Vista 1500 System (Siemens Healthcare Diagnostics) for liver enzymes, total cholesterol and triglycerides. Insulin and β-hydroxybutyrate were determined with a mouse insulin ELISA kit (80-INSMS-E01, ALPCO) and β-hydroxybutyrate assay kit (ab83390, Abcam), respectively. To assess autophagy induction by 3PO in vivo, GFP-LC3#53 transgenic mice[16] were treated with 3PO (50 mg/kg, i.p., 4x/week) or vehicle (DMSO). After 2 weeks, the autophagic flux inhibitor chloroquine was administered (50 mg/kg, i.p.) and mice were sacrificed 3 hours later using an overdose of sodium pentobarbital (250 mg/kg, i.p.). Liver and heart samples were isolated for immunohistochemical detection of LC3.

For atherosclerosis studies, 3PO (50 mg/kg, i.p.) or solvent (DMSO) was administered to female WD-fed ApoE$^{-/-}$Fbn1$^{C1039G+/-}$ mice, starting either after 4 weeks WD (2x/week, 10 weeks, preventive regimen) or after 16 weeks WD (4x/week, 4 weeks, curative regimen)(Supplemental Figure I). Female mice were chosen because the Fbn1 mutation frequently leads to aortic dissection in male ApoE$^{-/-}$Fbn1$^{C1039G+/-}$ mice, but not in female ApoE$^{-/-}$Fbn1$^{C1039G+/-}$ mice.[13] In addition, ApoE$^{-/-}$ mice on WD were treated with 3PO as described above (preventive regimen) to test the effects of 3PO on plaque size and composition in the absence of IP neovascularization. All animal procedures were conducted according to the guidelines for experimental atherosclerosis studies described in a scientific statement of the American Heart Association and the ATVB Council.[17, 18] Experiments were approved by the ethics committee of the University of Antwerp.

Histology

After euthanasia, the proximal aorta, aortic arch, carotid artery and heart were collected. Tissues were fixed in 4% formalin for 24 hours, dehydrated overnight in 60% isopropanol and subsequently embedded in paraffin. The plaque formation

index in ApoE$^{-/-}$Fbn1$^{C1039G+/-}$ mice was calculated on longitudinal sections of the carotid artery by using the following formula: (∑ total plaque length/∑ total vessel length) x100. Because plaques of ApoE$^{-/-}$ mice are less advanced as compared to ApoE$^{-/-}$Fbn1$^{C1039G+/-}$ mice, the plaque formation index in ApoE$^{-/-}$ mice was measured on longitudinal sections of the aortic arch (instead of the carotid artery). Haematoxylin-eosin (HE) staining was performed on cross-sections of the carotid artery of ApoE$^{-/-}$Fbn1$^{C1039G+/-}$ mice to analyse plaque thickness and percentage necrosis. The plaque thickness was assessed by taking the mean value of 10 random measurements in the respective area. Necrosis was defined as acellular areas filled with necrotic clefts and necrotic debris. Immunohistochemical staining for von Willebrand factor (anti-vWF, PC054, Binding Site) and Ter-119 (anti-Ter-119, 550565, BD Biosciences) were performed to detect plaque ECs and erythrocytes, respectively. Autophagosome formation in liver and heart of 3PO-treated GFP-LC3 mice was measured via LC3 immunostaining using rabbit anti-LC3 antibody (3868S, Cell Signaling). Plaque composition was analysed with Sirius red and anti-α-SMC actin (A2547, Sigma-Aldrich) staining to detect collagen and vascular smooth muscle cells, respectively. Macrophages and macrophage polarization were examined by immunohistochemistry using anti-MAC3 (01781D, Pharmingen) and antibodies against M1/M2 markers (anti-Egr2, PA5-27814, ThermoFisher Scientific; anti-GPR18, PA5-23218, ThermoFisher Scientific; anti-Arg-1, PA5-29645, ThermoFisher Scientific; anti-CD38, MBS129421, MyBioSource). Quantification of immunstains was done from 10 random images per section using ImageJ software. The occurrence of myocardial infarctions (defined as large fibrotic areas) and coronary plaques was analysed on Masson's trichrome staining (transversal sections). Expression of adhesion molecule VCAM-1 was analysed using anti-VCAM-1 (ab134047, Abcam). *En face* Oil Red O staining was performed on the carotid artery and aortic arch of ApoE$^{-/-}$Fbn1$^{C1039G+/-}$ mice.

Echocardiography

Transthoracic echocardiograms were performed on anesthetized mice (isoflurane, 4% for induction and 2.5% for maintenance) at the end of the experiment using a VEVO2100 (VisualSonics), equipped with a 25 MHz transducer. Left ventricular

internal diameter during diastole (LVIDd) and left ventricular internal diameter during systole (LVIDs) were measured and fractional shortening [FS = (LVIDd-LVIDs)/LVIDd*100] was calculated.

Cell culture

Human aortic endothelial cells (HAOECs; Sigma-Aldrich) were cultured in Endothelial Cell Growth Medium (PromoCell) supplemented with 2% fetal bovine serum, 0.4% endothelial cell growth supplement, 0.1 ng/ml epidermal growth factor, 1 ng/ml basic fibroblast growth factor, 90 µg/ml heparin and 1 µg/ml hydrocortisone. To investigate the expression of VCAM-1 and ICAM-1, HAOECs were stimulated with 20 ng/ml human TNF-α. A transcription factor assay kit was used to detect the NF-κB transcription factor DNA binding activity in nuclear extracts according to the manufacturer's instructions (ab133112, Abcam). For siRNA-mediated silencing of the autophagy pathway, HAOECs were seeded into 6-well plates and transfected at 75% confluency with 2.5 ml Opti-MEM Reduced Serum Medium (Thermo Fisher) containing 40 nM ATG7 siRNA (Dharmacon) and 2.5 µl Lipofectamine RNAiMAX (Thermo Fisher) for 6 hours.

Real-time RT-PCR

Total RNA was isolated using an Isolation II RNA mini kit (Bioline) according to the manufacturer's instructions. Reverse transcription was performed with a Sensifast™ cDNA Synthesis Kit (Bioline). Thereafter, Taqman gene expression assay (Applied Biosystems) for CD38 (assay ID: Mm01220906_m1), Gpr18 (assay ID: Mm01224541_m1), Egr2 (assay ID: Mm00456650_m1) and Arg1 (assay ID: Mm00475988_m1) were performed in duplicate on an ABI prism 7300 sequence detector system (Applied Biosystems). The parameters for PCR amplification were 95°C for 10 minutes followed by 40 cycles of 95°C for 15 seconds and 60°C for 1 minute. Relative expression of mRNA was calculated using the comparative threshold cycle method. All data were normalized for quantity of cDNA input by performing measurements on the endogenous reference gene β-actin.

Western Blot analyses

Cells were lysed in an appropriate volume of Laemmli sample buffer (Bio-Rad) containing β-mercaptoethanol (Sigma-Aldrich) and boiled for 5 min. Protein samples were then loaded onto pre-casted Bolt 4-12% Tris-Bis gels (Invitrogen) and after electrophoresis transferred to Immobilon-FL PVDF membranes (Millipore) according to standard procedures. Membranes were blocked for 1 hour with Odyssey blocking buffer (LI-COR Biosciences) diluted 1:5 with PBS. After blocking, membranes were probed overnight at 4°C with primary antibodies diluted in Odyssey blocking buffer, followed by 1 hour incubation with IRDye-labeled secondary antibodies at room temperature. Antibody detection was achieved using an Odyssey SA infrared imaging system (LI-COR Biosciences). The intensity of the protein bands was quantified using Image Studio software. The following primary antibodies were used: anti-β-actin (ab8226, Cell Signaling), anti-mTOR (2972, Cell Signaling), anti-phospho-mTOR (S2448) (2971, Cell Signaling), anti-p70 S6 Kinase (9202, Cell Signaling), anti-phospho-p70 S6 Kinase (Thr389) (9205, Cell Signaling), anti-LC3 (clone 5F10, 0231-100/LC3-5F10, Nanotools), anti-VCAM-1 (ab134047, Abcam), anti-ATG7 (8558S, Cell Signaling), anti-NF-κB (8242, Cell Signaling), anti-phospho-NF-κB (3039, Cell Signaling) and anti-ICAM-1 (ab179707, Abcam). IRDye-labelled secondary antibodies (goat anti-mouse IgG, 926-68070, and goat anti-rabbit IgG, 926-32211) were purchased from LI-COR Biosciences.

Transmission electron microscopy

Tissue samples were fixed in 2.5% glutaraldehyde, 0.1M sodium cacodylate and 0.05% $CaCl_2$ (pH 7.4) and further processed for transmission electron microscopy as described previously,[19] with a minor modification (extra staining with 1% tannic acid in veronal acetate for 1 hour after OsO4 postfixation). A FEI Tecnai microscope was used to examine ultrathin sections at 80-120 kV. Autophagic vacuoles were quantified on 5 different images taken at random per section.

Statistics

All data are expressed as mean ± SEM. Statistical analyses were performed using SPSS software (version 25, SPSS Inc.). Statistical tests are specified in the figure and table legends. When parametric statistics (ANOVA, Student's t-test) were used, a test of normality (Shapiro-Wilk test) and a test for equal variances (Levene's test) were performed. In every case, the data passed normality and equal variance tests. If not, non-parametric statistics (Mann-Whitney U test, Kruskal-Wallis test) were used. A Chi-square test was used to determine whether there was an association between categorical variables (i.e., whether the variables are independent or related). A Fisher's exact test was used when sample sizes were small (i.e. when one of the four cells of a 2x2 table had less than five observations) to test whether two categorical variables were associated with each other or not. A Mann-Whitney U test was used to compare differences between two independent groups when the dependent variable was either ordinal or continuous, but not normally distributed. A Kruskal-Wallis test was used as an alternative for a one-way ANOVA if the assumptions of the latter were violated (i.e. data not normally distributed and/or unequal variances). Differences were considered significant at $p<0.05$.

Results

3PO is not toxic, but causes a metabolic switch in mice

To evaluate whether glycolysis inhibitor 3-(3-pyridinyl)-1-(4-pyridinyl)-2-propen-1-one (3PO) affects general metabolism, female ApoE$^{-/-}$ mice were fed a western-type diet and treated with 3PO (50 mg/kg, i.p., 4x/week) or vehicle for 4 weeks. Plasma analysis did not reveal changes in the level of liver enzymes (GTT, ALT, ALP), fasting and non-fasting blood glucose, insulin or total cholesterol (Table 1). Moreover, according to a glucose and insulin tolerance test, glucose absorption and insulin receptor sensitivity were not different in 3PO-treated mice as compared to vehicle-treated controls (Supplemental Figure II). Experiments in metabolic cages showed that water intake was not altered, though food consumption significantly decreased in 3PO-treated mice (P=0.0002, Table 1). Also body weight tended to decrease, though this effect was not statistically significant (P=0.1241). Levels of plasma

triglycerides clearly decreased (*P*=0.0086), whereas those of ketone body β-hydroxybutyrate increased (*P*=0.0443, Table 1). Because starvation is a well-known trigger of autophagy induction, we evaluated whether reduced food intake after 3PO treatment stimulates autophagy in liver and heart, which are one of the most sensitive organs to starvation-induced autophagy.[16] Unlike complete food withdrawal that strongly evoked autophagy, autophagosome staining was negative in liver and heart of 3PO treated GFP-LC3 mice (supplemental Figure III).

Table 1. Metabolic parameters of ApoE$^{-/-}$ mice treated for 4 weeks with 3PO or vehicle (DMSO)

Metabolic parameters	Control	3PO
Liver enzymes		
- γ-glutamyltransferase (U/L)	11 ± 1	9 ± 1
- Alanine transaminase (U/L)	34 ± 6	29 ± 6
- Alkaline phosphatase (U/L)	174 ± 10	130 ± 20
Fasting blood glucose (mg/dL)	85 ± 3	81 ± 4
Non-fasting blood glucose (mg/dL)	186 ± 5	171 ± 10
Insulin (ng/ml)	0.2 ± 0.1	0.2 ± 0.1
Total cholesterol (mg/dL)	599 ± 1	563 ± 20
Food intake (g/day)	2.6 ± 0.1	1.7 ± 0.1***
Water intake (ml/day)	4.1 ± 0.3	3.4 ± 0.5
Body weight (g)	20.3 ± 0.4	19.4 ± 0.3
Triglycerides (mg/dL)	93 ± 7	65 ± 7**
β-hydroxybutyrate (μM)	8 ± 1	12 ± 1*

3PO was administered at 50 mg/kg (i.p.; 4x/week) for 4 weeks. Data shown as mean ± SEM. **P*<0.05, ***P*<0.01, ****P*<0.001 versus control (unpaired Student *t* test, n=10-12).

3PO inhibits neovascularization in plaques of ApoE$^{-/-}$Fbn1$^{C1039G+/-}$ mice

3PO (50 mg/kg, i.p.) or vehicle was administered to ApoE$^{-/-}$ Fbn1$^{C1039G+/-}$ mice starting either after 4 weeks western-type diet (WD; 2x/week, 10 weeks, preventive regimen) or after 16 weeks WD (4x/week, 4 weeks, curative regimen). As shown by anti-VWF staining of plaques in the carotid arteries of ApoE$^{-/-}$Fbn1$^{C1039G+/-}$ mice, 3PO reduced the number of mice with IP neovascularization with almost 40% (curative regimen) and 50% (preventive regimen) (Figure 1A). Moreover, the number of microvessels per plaque significantly decreased (Figure 1A). IP microvessels were not observed in the proximal aorta. An anti-Ter-119 staining showed that microvessels were leaky and released erythrocytes into the plaque (Figure 1B). The number of IP haemorrhages was reduced after treatment with 3PO in the preventive setting (control= 2.25 [0.0-7.0]/; 3PO= 0.00 [0.0-3.0]/mm^2; *P*=0.03). A decrease in the number of IP haemorrhages was also observed in a curative 3PO regimen, though this effect was not significant (control= 9.57 [0.0-25.53]; 3PO= 0.0 [0.0-23.09]/mm^2; *P*=0.46).

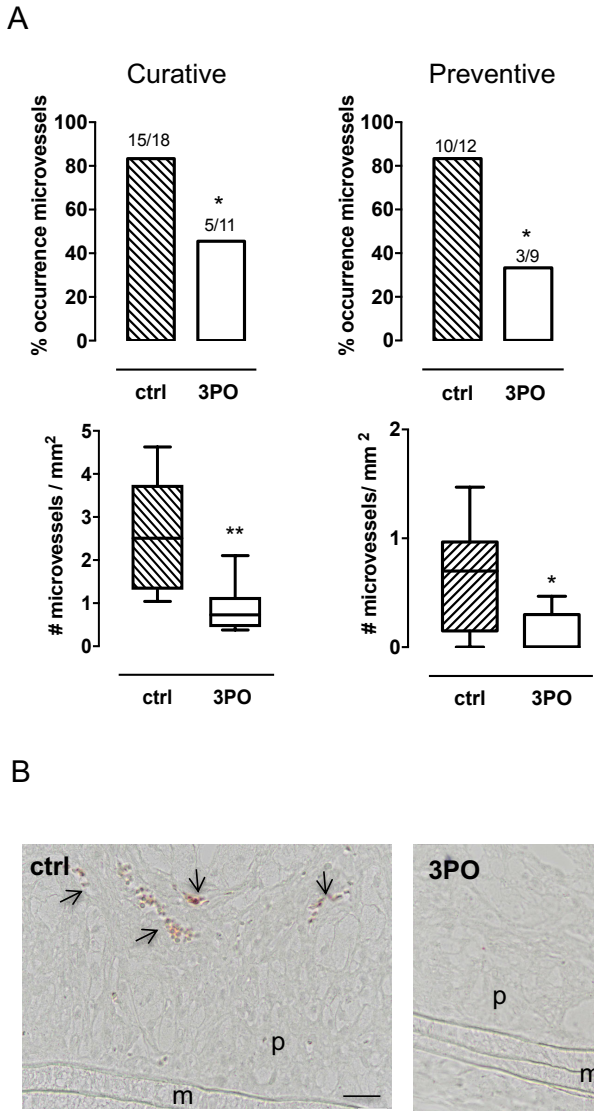

Figure 1. 3PO inhibits intraplaque neovascularization in the carotid artery of ApoE$^{-/-}$ Fbn1$^{C1039G+/-}$ mice. (A) Differences in the occurrence (number of mice) and the number of intraplaque microvessels of control (ctrl) and 3PO-treated mice that underwent a curative or preventive 3PO regimen. **P*<0.05, ***P*<0.01 versus ctrl (Chi-square (upper panels) or Mann-Whitney U test (lower panels); control: n=8-10, 3PO: n=9-13). (B) Anti-Ter-119 staining of atherosclerotic plaques in the carotid artery of control (ctrl) and 3PO-treated mice (curative regimen). Microvessels are marked by arrows. M=media, P=plaque. Scale bar = 50 µm.

3PO inhibits atherosclerotic plaque formation independent of IP neovascularization and without affecting plaque composition

An analysis of total cholesterol did not reveal significant differences between 3PO-treated ApoE$^{-/-}$Fbn1$^{C1039G+/-}$ mice and untreated controls (curative regimen: 507 ± 58 vs 602 ± 58 mg/dl; preventive regimen: 454 ± 24 vs 527 ± 33 mg/dl). 3PO did not change plaque thickness and plaque necrosis (Table 2, Supplemental Figure IV). Moreover, the smooth muscle cell and macrophage content of plaques as well as the percentage of total plaque collagen was not different between control and 3PO-treated animals (Table 2, Supplemental Figure IV). Nonetheless, plaque formation was reduced in both the curative regimen and preventive regimen as illustrated by the plaque formation index (Figure 2A) and *en face* oil-red O stainings (Figure 2B). Importantly, ApoE$^{-/-}$Fbn1$^{C1039G+/-}$ mice that contained plaques without obvious IP neovascularization revealed similar inhibition of plaque formation (Figure 2A), suggesting that 3PO may control atherosclerotic plaque formation independent of IP microvessel growth. In line with this finding, 3PO was able to inhibit plaque formation in the aortic arch of regular ApoE$^{-/-}$ mice that do not develop IP neovascularization (control= 53.9 ± 4.8 %; 3PO=38.6 ± 5.2 %, *P*=0.04).

Table 2. Thickness and composition of atherosclerotic plaques in the carotid artery of ApoE$^{-/-}$Fbn1$^{C1039G+/-}$ mice

	Curative		*Preventive*	
	Control	3PO	Control	3PO
Plaque thickness (µm)	316 ± 13	312 ± 27	314 ± 27	262 ± 12
Necrosis (%)	13 ± 1	14 ± 3	7 ± 1	7 ± 2
Smooth muscle cells (%)	8 ± 1	9± 1	7 ± 2	6 ± 1
Macrophages (%)	7 ± 1	5 ± 1	12 ± 4	8 ± 2
Collagen (%)	26 ± 2	25 ± 2	16 ± 1	15 ± 4

Data shown as mean ± SEM, n=10-16; Curative=4 weeks treatment (weeks 16-20 on western-type diet), preventive=10 weeks treatment (weeks 4-14 on western-type diet). Unpaired Student *t* test: not significant.

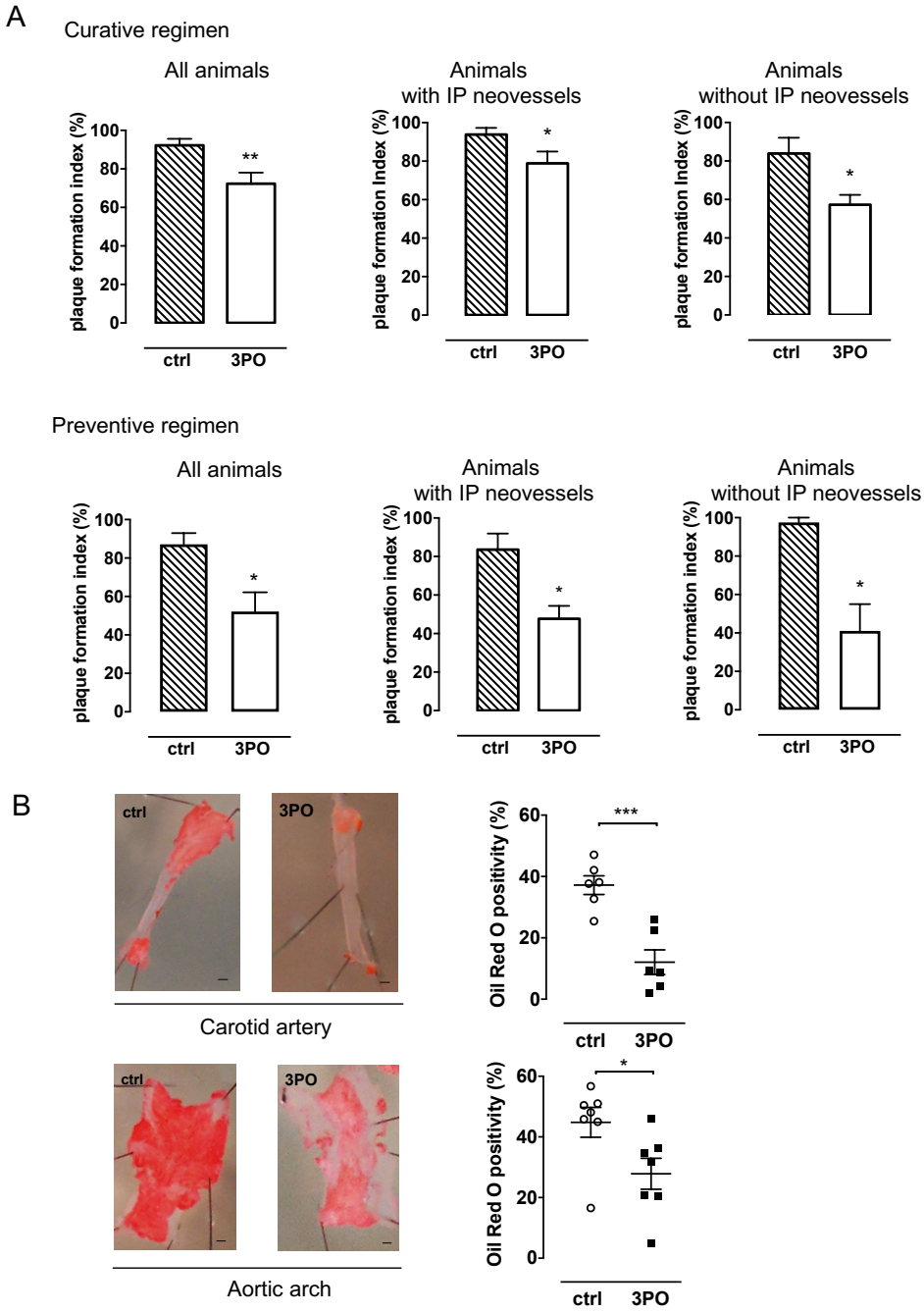

Figure 2. 3PO inhibits atherosclerotic plaque formation in ApoE$^{-/-}$Fbn1$^{C1039G+/-}$ mice. (A) Plaque formation index of the right carotid artery as a measure of plaque occurrence in control (ctrl) and 3PO-treated mice that underwent a curative or preventive 3PO regimen. Plaque

formation index is shown for all animals (left panel) of the control (crtl) group (n=12) and 3PO-treated group (n=9), for mice with intraplaque microvessels (middle panel; 10/12 control mice and 3/9 treated mice) or for mice without intraplaque microvessels (right; 2/12 controls and 6/9 treated mice). *P<0.05, **P<0.01 versus ctrl (Mann-Whitney U test). (B) En face Oil Red O staining of the carotid artery and aortic arch of control (n=6-7) and 3PO-treated vessels (n=6-7). Scale bar = 1.5 mm. *P<0.05, ***P<0.001 versus ctrl (Independent samples t-test).

3PO has a positive impact on cardiac function when administered in a preventive manner

Unlike standard ApoE$^{-/-}$ mice or ApoE$^{-/-}$Fbn1$^{C1039G+/-}$ mice on normal laboratory diet, ApoE$^{-/-}$Fbn1$^{C1039G+/-}$ mice on western-type diet develop (sometimes highly stenotic) coronary artery plaques, which negatively affect the heart.[13] Therefore, cardiac function and structure were assessed in ApoE$^{-/-}$Fbn1$^{C1039G+/-}$ mice after 3PO treatment via echocardiography and histology, respectively. In the curative setting, measurements of the left ventricular internal diameter during diastole (LVIDd) (control= 4.6 ± 0.2 µm; 3PO= 4.5 ± 0.2 µm) and the left ventricular internal diameter during systole (LVIDs) (control= 3.5 ± 0.2 µm; 3PO= 3.2 ± 0.3 µm) did not show significant differences between control and treated animals. The fractional shortening (FS) was also similar between both groups (control= 23.1 ± 3.0; 3PO= 29.3 ± 3.7 µm). However, the ratio heart weight/body weight was significantly different between 3PO-treated animals and controls (control= 9.8 ± 0.8 %; 3PO= 6.9 ± 0.3 %, P=0.0081). The preventive regimen resulted in significantly smaller LVIDs and LVIDd with an increased FS (Supplemental Figure VA-D). Analysis of fibrotic areas on heart sections did not show a decrease in the occurrence of myocardial infraction (Fisher's exact test, curative= ctrl 2/15 vs 3PO 2/12; P=1.00; preventive= ctrl 2/10 vs 3PO 0/9; P=0.47). The number of mice with coronary plaque formation tended to decrease in the curative setting (Fisher's exact test, ctrl 12/14 mice vs 3PO 7/12 mice; P=0.19). It was not significant in the preventive setting, even though a 50% decrease in the occurrence of coronary plaque formation was observed in animals after 10 weeks of treatment (Fisher's exact test, ctrl 6/10 mice vs 3PO 3/9 mice, P=0.36). Further analysis of coronary arteries (in preventive regimen) showed

that perivascular fibrosis decreased after treatment with 3PO (supplemental Figure VE).

3PO increases the number of autophagosomes in EC

3PO is a glycolysis inhibitor that leads to moderate ATP depletion.[9] To investigate whether this metabolic stress condition triggers autophagy, human aortic endothelial cells were stimulated in vitro with 3PO for 16 hours. Levels of the autophagosomal marker protein LC3-II increased in a concentration-dependent manner (Figure 3A), and stimulated formation of autophagic vesicles as shown by transmission electron microscopy (Figure 3B). In contrast to the well-known autophagy inducer everolimus that stimulates autophagy via mTOR inhibition, the phosphorylation status of mTOR or its downstream substrate p70S6K was not affected by 3PO (Figure 3C).

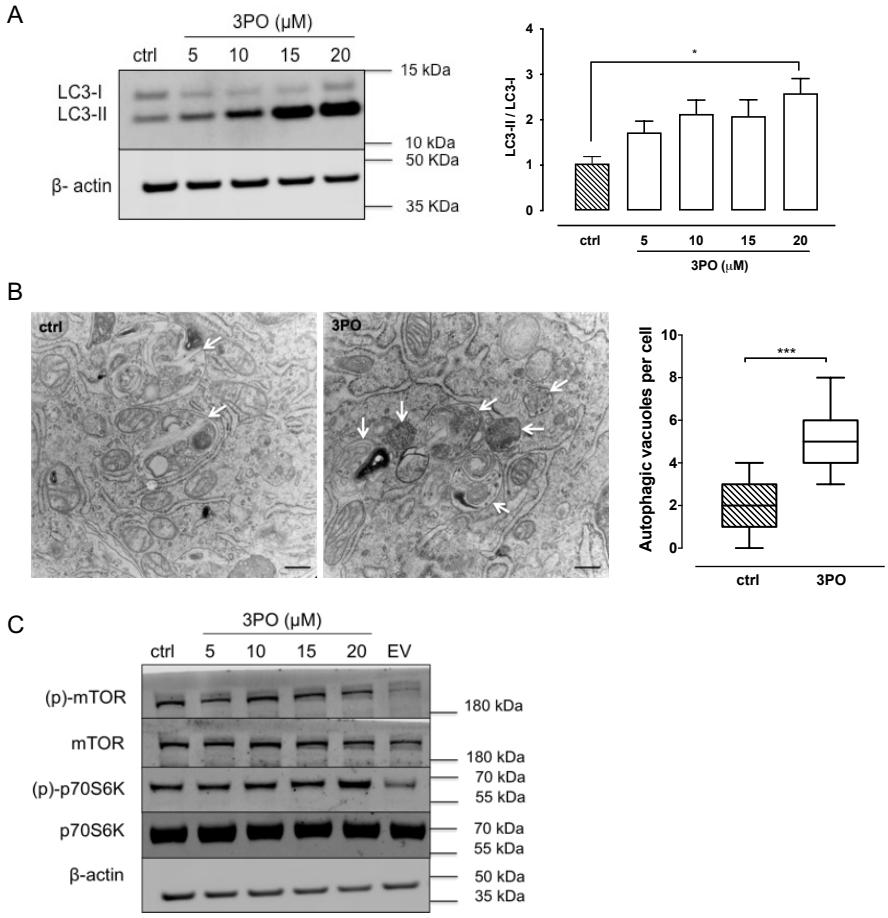

Figure 3. 3PO stimulates autophagosome formation in endothelial cells independent of mTOR. (A) Human aortic endothelial cells (HAOECs) were stimulated with 3PO (5-20 μM) for 16 hours followed by western blot analysis for the autophagosomal marker protein LC3. Protein levels of LC3-I and LC3-II were quantified relative to the reference protein β-actin. **P*<0.05 versus untreated control cells (ctrl) (1-way ANOVA, followed by Dunnett test, n=3). (B) Detection and quantification of autophagic vacuoles (arrows) in 3PO-treated HAOECs (20 μM 3PO, 16 hours) using transmission electron microscopy. Scale bar = 500 nm. ****P*<0.001 (Mann-Whitney U test; n=3). (C) Evaluation of the phosphorylation status of mTOR and its downstream target p70S6K in 3PO-treated HAOECs via western blotting. Everolimus (EV, 10 μM) was used as a positive control.

3PO reduces endothelial VCAM-1 expression in an autophagy-dependent way

One of the early steps in plaque formation is up-regulation of adhesion molecules such as VCAM-1 followed by monocyte infiltration.[20, 21] Because 3PO inhibits plaque formation, we investigated whether VCAM-1 expression could be inhibited by 3PO. To this end, human aortic endothelial cells were stimulated with TNF-α in the presence or absence of 3PO. TNF-α treated cells clearly upregulated VCAM-1 and ICAM-1 protein expression, yet upregulation of both proteins was significantly impaired in the presence of 3PO (Figure 4). Moreover, NF-κB signalling was blunted by 3PO, given the significantly lower levels of phosphorylated NF-κB and a reduced DNA binding activity of NF-κB in 3PO-treated cells (Supplemental Figure VI). Silencing of the essential autophagy gene ATG7 promoted VCAM-1 and ICAM-1 expression and could neither be enhanced by TNF-α nor inhibited by 3PO (Figure 4). $ApoE^{-/-}Fbn1^{C1039G+/-}$ and $ApoE^{-/-}$ mice treated with 3PO (preventive regimen) revealed a decreased expression of VCAM-1 at the luminal EC surface of the plaque (Figure 4).

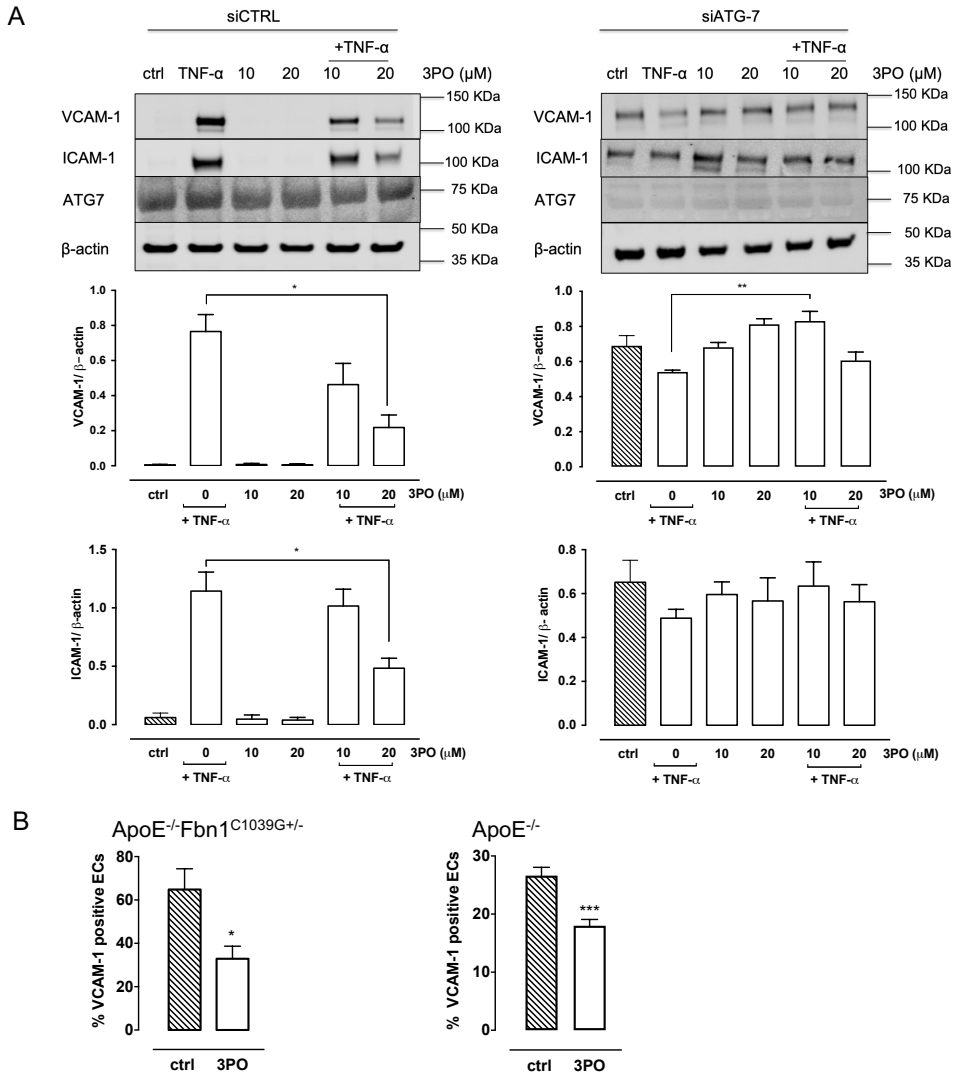

Figure 4. 3PO impairs TNF-α mediated upregulation of VCAM-1 and ICAM-1 in endothelial cells via autophagy. (A) qPCR and western blot analysis of VCAM-1, ICAM-1 and ATG7 expression, either in wild type (siCTRL-treated) human aortic endothelial cells (HAOECs; left panels) or siATG7-treated HAOECs (right panels), and exposed to hTNF-α (20 ng/ml) in the presence or absence of 3PO (10-20 μM) for 24 hours. β-actin was used as a reference gene. **P*<0.05, ***P*<0.01 (1-way ANOVA followed by Dunnett test, n=3). (B) Quantification of VCAM-1 positive endothelial cells in the carotid artery of ApoE$^{-/-}$Fbn1$^{C1039G+/-}$ and the aortic arch of ApoE$^{-/-}$ mice treated with 3PO or solvent (ctrl) for 10 weeks (preventive regimen). **P*<0.05, ****P*<0.001 versus ctrl (unpaired Student *t* test, n=7-12).

3PO promotes an M2 macrophage subtype in vitro

Because 3PO regulates inflammation and may affect macrophage polarization,[22] gene expression of M1 and M2 exclusive genes[23] was analysed *in vitro* by real-time PCR in 3PO-treated mouse macrophages. 3PO did not change gene expression of M1 genes CD38 and Gpr18, but significantly upregulated expression of M2 genes Egr2 and Arg1 in a concentration-dependent manner (Figure 5). Furthermore, stimulation of an M1 phenotype by IFN-γ/LPS was inhibited by 3PO (Figure 5). Because of aspecific and unreliable antibody staining, the abovementioned M1/M2 markers failed to translate to macrophages in plaques of vehicle- or 3PO-treated carotid arteries and confirms recent statements in literature that valid *in vivo* M1/M2 surface markers remain to be discovered.[24]

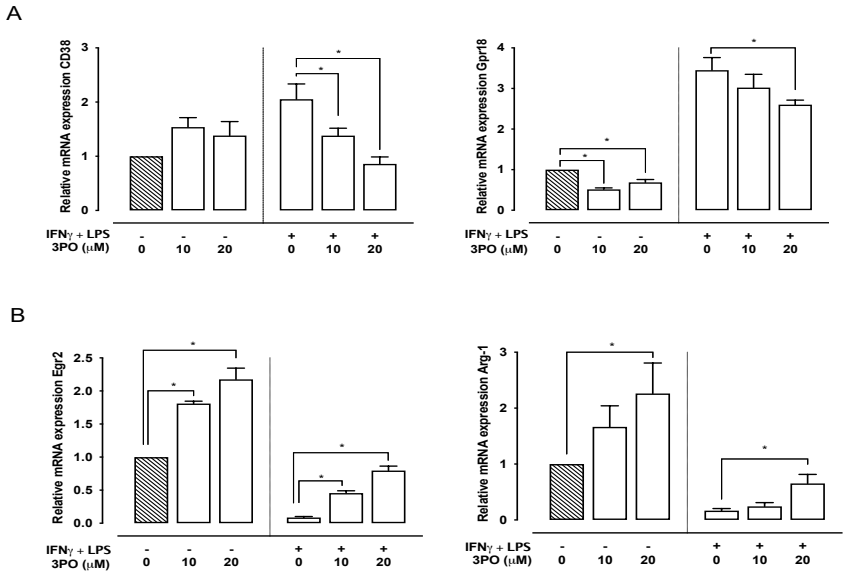

Figure 5. 3PO promotes a macrophage M2 phenotype. Bone marrow derived macrophages from ApoE$^{-/-}$ mice were treated in vitro with 3PO (10-20 μM) and/or a mixture of IFN-γ (20 ng/ml) and LPS (100 ng/ml) for 24 hours. Subsequently, mRNA expression of M1 exclusive genes CD38 and Gpr18 (A) or the M2 specific genes Erg2 and Arg-1 (B) was analyzed by real time PCR. **P*<0.05 (Kruskal-Wallis followed by Mann-Whitney U test, n=4).

Discussion

There is an obvious association between IP neovascularization and plaque vulnerability in advanced human plaques.[25] However, the causality and impact of IP neovascularization on plaque destabilization is poorly studied. In oncology, research is far more ahead on this topic and several anti-angiogenic strategies have been tested in an experimental set-up.[26] To date, blocking VEGF was the primary strategy for reducing neovascularization.[27, 28] Unfortunately, limited efficacy and adverse effects have been downsizing its success, even when multiple blockers were used simultaneously.[5, 29] Therefore, a fundamentally different approach is required to re-boost anti-angiogenic therapies. Given that ECs rely on glycolysis for up to 85% of their energy demand,[7] targeting EC metabolism may represent an attractive new strategy to inhibit neovascularization.[8, 30] Transient and partial inhibition of glycolysis in proliferating ECs by the small molecule 3PO inhibits pathological angiogenesis without interfering with the metabolism of healthy cells.[9] In line with this statement, experimental evidence from the present study indicates that treatment of $ApoE^{-/-}$ mice with 3PO for 4 weeks caused neither substantial adverse effects nor changes in general metabolism. Reduced food intake was observed, yet circulating liver enzymes, blood glucose, insulin and total cholesterol were not affected. Also a glucose and insulin tolerance test was perfectly normal. However, 3PO caused a decrease in the level of circulating triglycerides and a significant rise in β-hydroxybutyrate levels, indicating a metabolic switch from glucose to fatty acid-derived ketones in order to provide sufficient energy. Lack of major side effects was also reported recently by Beldman et al.[31] after treatment of atherosclerotic $ApoE^{-/-}$ mice for 6 weeks with 3PO (25 mg/kg, i.p., 3x/week).

Once safe administration of 3PO was evident, we next investigated the effect of 3PO on the formation of IP microvessels in a mouse model of advanced atherosclerosis (i.e. $ApoE^{-/-}$ mice with a heterozygous mutation in the fibrillin-1 gene [$Fbn1^{C1039G+/-}$], yielding large plaques with a highly unstable phenotype and extensive IP neovascularization).[13] Analysis of IP neovascularization in the carotid artery revealed a significant decrease in the occurrence and the amount of microvessels in $ApoE^{-/-}Fbn1^{C1039G+/-}$ mice treated with 3PO. These results are in line with the effect of 3PO in cancer tissue, where 3PO inhibits vascular sprouting in pathological

angiogenesis.[7] Because inhibition of angiogenesis in malignant tissue can affect tumor growth,[32] it was interesting to investigate the impact of 3PO on plaque size and vulnerability. After 4 weeks of treatment, we could not observe a difference in plaque composition between control and treated animals. These results fed the presumption that even though 4 weeks of treatment is enough to inhibit IP neovascularization, it may have been too short to have any impact on plaque size or composition. Therefore, we decided to repeat the experiment in a preventive manner with 3PO being administered over a longer period of time. Given that i.p. injections are very stressful for ApoE$^{-/-}$Fbn1$^{C1039G+/-}$ mice, they were injected with 3PO for a maximum of 10 weeks.[33] The preventive treatment regimen confirmed the results that we obtained after the curative treatment regimen with an even larger decrease in IP neovascularization. Nonetheless, we could not observe a difference in parameters defining plaque vulnerability such as changes in macrophages, smooth muscle cells and total collagen. Because IP microvessels are considered a potential entry site for erythrocytes, lipids and inflammatory mediators in the plaque,[34, 35] it was highly unexpected that, after 10 weeks of treatment, plaque composition was similar between control and treated animals.

Importantly, although the plaque size and composition remained unchanged, the occurrence of plaques as measured by the plaque formation index was significantly reduced in 3PO-treated animals. After 10 weeks of treatment, a 35% reduction in plaque formation was observed in the carotid artery. Given that neovascularization occurs after a certain degree of hypoxia, plaque progression is already in an advanced state. A decrease in the plaque formation index demonstrates that EC metabolism plays an important role in the early stages of plaque development, apart from angiogenesis. Indeed, a 3PO-mediated reduction in plaque development was also observed in regular ApoE$^{-/-}$ mice, which develop plaques without IP neovascularization. When ECs undergo inflammatory activation, the upregulation of adhesion molecules such as VCAM-1 represents an important trigger in early lesion development, as they attract and encourage monocytes to enter the lesion.[36] In the present study, we provide in vitro and in vivo evidence that 3PO interferes with the upregulation of VCAM-1 and ICAM-1. In vitro experiments with ECs, pre-activated with TNF-α and treated with 3PO, revealed impaired NF-κB signalling and reduced VCAM-1 (and ICAM-1) expression levels. Moreover, a preventive 3PO regimen was

able to reduce VCAM-1 expression in the endothelium in vivo. A study performed in cancer research consolidates these results as 3PO reduced the expression of adhesion molecules concomitant with tumour vessel normalization due to an altered EC pro-inflammatory signature.[37] Nonetheless, the question remains why changes in VCAM-1 expression in 3PO-treated mice do not alter plaque composition. Our data seem to suggest that 3PO only impairs initiation of plaque development, but not plaque progression. Indeed, one may speculate that once early plaques have formed, downregulation of VCAM-1 expression in ECs by 3PO does not significantly affect further leukocyte recruitment and plaque progression. Histological data from human plaques indicate that in early lesions VCAM-1 and ICAM-1 are predominantly expressed by the endothelium, whereas in more advanced lesions, the majority of VCAM-1 expression is found in subsets of intimal VSMCs and macrophages.[38] These findings may explain why downregulation of adhesion molecules by 3PO in ECs mainly affects the initial stage of atherosclerosis development, but not further steps of plaque progression.

Interestingly, the metabolic stress caused by 3PO stimulated autophagosome formation in ECs and led to induction of autophagy. Similar observations were previously reported in cancer cells.[39] Our results indicate that downregulation of endothelial VCAM-1 (and ICAM-1) expression by 3PO depends on autophagy induction. Expression of the adhesion molecules was not downregulated by 3PO in TNF-α-treated ECs in which expression of the essential autophagy gene ATG7 was silenced. On the contrary, VCAM-1 (and ICAM-1) expression was upregulated in ATG7-deficient ECs, suggesting that autophagy suppresses expression of these adhesion molecules. Previously, we reported similar data with the biguanide metformin. The latter compound attenuates expression of the endothelial cell adhesion molecules ICAM-1 and VCAM-1 as well as formation of atherosclerotic plaques via autophagy induction.[40] Downregulation of ATG7 gene expression prevented TNF-α induced upregulation of VCAM-1 expression and monocyte adhesion to ECs. Both metformin and 3PO govern the expression of cell adhesion molecules in ECs by inhibiting NF-κB activation. Our findings support previous data showing that endothelial autophagy is atheroprotective and limits atherosclerotic plaque formation by preventing endothelial apoptosis, senescence and inflammation.[41-43]

Apart from the atheroprotective effects on ECs, several lines of evidence indicate that 3PO also negatively influences inflammation.[22, 31, 44-46] In the present study, we could demonstrate that 3PO favors an anti-inflammatory M2 macrophage subtype and suppresses an M1 pro-inflammatory phenotype *in vitro*. This finding is consistent with previous reports showing a strong linear correlation between glycolytic flux and proinflammatory activation of macrophages (as measured by TNF-α production)[22] and 3PO-mediated suppression of T cell activation.[44] Moreover, inhibition of glycolysis by 3PO has profound effects on cell viability of M1 macrophages.[22]

Given the importance of neovascularization in the ischemic myocardium after an acute myocardial infarction, we analysed cardiac function and morphology.[47] The inhibition of angiogenesis by targeting cell metabolism is still in a preclinical stage, thus literature regarding this topic is still lacking. After a curative treatment regimen, no significant differences were observed in cardiac function. However, after 10 weeks of treatment (preventive regimen), we observed an improved cardiac morphology and function (smaller LVIDs and LVIDd with increased fractional shortening). Moreover, even though only a small non-significant reduction was observed in the occurrence of myocardial infarctions, the occurrence of coronary plaques was decreased by 50% in treated animals. These findings are consistent with the overall effect of 3PO on plaque formation, in this case coronary plaques. As such, it is conceivable that the overall improved cardiac function is a result of less coronary plaque formation. To further explain the improved cardiac function after 3PO treatment (preventive regimen), we also documented the level of perivascular fibrosis of coronary arteries. This parameter was significantly reduced by 3PO. Because coronary perivascular fibrosis can be caused by an impaired coronary blood flow,[48] a lower degree of stenosis in the coronary arteries of 3PO treated mice probably contributes to this finding. Similar observations were recently made in the same mouse model using lipid lowering therapy.[49] Apart from improved cardiac function through less coronary plaque formation and coronary perivascular fibrosis, it is important to note that autophagy induction has beneficial effects on the heart.[50]Because 3PO promotes autophagy, it is plausible to assume that autophagy induction by 3PO also contributes to improved cardiac function. However, given the lack of autophagosome formation in 3PO-treated GFP-LC3 mice, we consider this hypothesis unlikely, though cannot completely rule out this possibility.

In conclusion, we were able to inhibit IP neovascularization with 3PO. However, the reduction in IP microvessels did not exert a significant effect on plaque composition. Surprisingly, 3PO reduced the formation of plaques, not in size but in frequency. Less plaques were formed in the carotid artery indicating that 3PO already has an effect in the early onset of atherosclerosis by downregulating endothelial cell adhesion molecules. In addition, fewer coronary plaques were formed, which resulted in overall improved cardiac function. Interestingly, inhibition of key steps in glycolysis with small molecules has recently provided a novel area of cancer research and has been proven effective in slowing the proliferation of cancer cells, with PFK158 as a first-in-human and first-in class PFKFB3 inhibitor in a phase I clinical trial (NCT02044861). Compared to cancer, the endothelial cell metabolism in atherosclerosis is largely unexplored, though is an emerging target that may offer attractive therapeutic avenues to counteract plaque progression.[8, 51, 52]

Acknowledgements

The authors would like to thank Dr. Bart Peeters, Sofie De Moudt, Anne-Elise Van Hoydonck, Hermine Fret and Rita Van den Bossche for technical help. The authors are grateful to Dr. Bronwen Martin for critical reading of the manuscript.

Sources of Funding

This work was supported by the University of Antwerp [DOCPRO-BOF], the Hercules Foundation [grant number AUHA/13/03] and the Horizon 2020 program of the European Union – Marie Sklodowska Curie actions – ITN – MOGLYNET [grant number 675527].

Supplemental Material

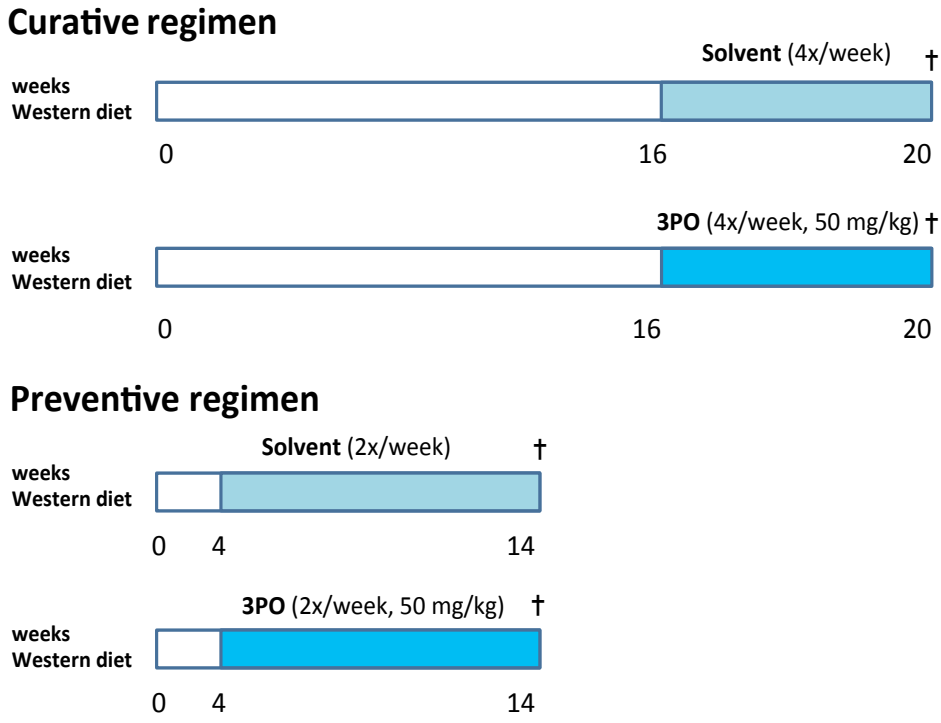

Figure I. Schematic overview of 3PO treatment regimens applied in ApoE$^{-/-}$Fbn1$^{C1039G+/-}$ mice. Mice were fed a western diet and received i.p. injections of 3PO (50 mg/kg) after 4 weeks of diet (preventive regimen, 2x/week) or after 16 weeks of diet (curative treatment regimen, 4x/week). The preventive regimen was also applied to ApoE$^{-/-}$ mice.

A

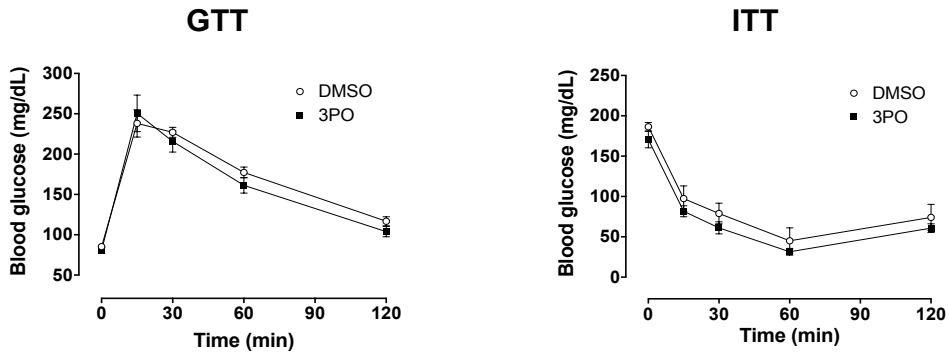

Figure II. Glucose clearance in 3PO- or vehicle-treated ApoE$^{-/-}$ mice after intraperitoneal injection with glucose or insulin. A glucose tolerance test (GTT) and insulin tolerance test (ITT) were performed in female ApoE$^{-/-}$ mice after 4 weeks of treatment with 3PO (50 mg/kg, i.p.; 4x/week) or vehicle. Blood glucose was measured at different time points after injection of glucose (1 g/kg, i.p.) or insulin (1 U/kg, i.p.). Two-way ANOVA: GTT, Time: P<0.001, 3PO: P=0.181, Interaction: P=0.708; ITT, Time: P<0.001, 3PO: P=0.083, Interaction: P=0.992

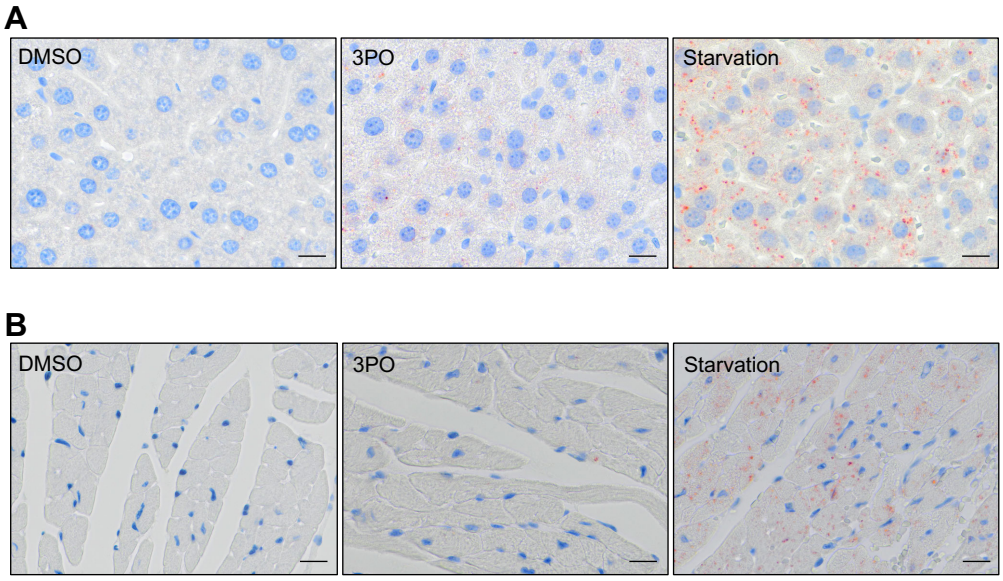

Figure III. Immunohistochemical analysis of autophagy induction in liver and heart of GFP-LC3 transgenic mice after treatment with 3PO or after starvation. GFP-LC3 mice were treated with 3PO (50 mg/kg, i.p., 4x/week) or vehicle (DMSO) for 2 weeks, or underwent nutrient deprivation (starvation) for 24 hours. Autophagic flux inhibitor chloroquine was administered (50 mg/kg, i.p.) 3 hours before the sacrification of mice. Liver (A) and heart samples (B) were isolated for immunohistochemical detection of autophagosomes using LC3 antibodies. Scale bar = 20 μm.

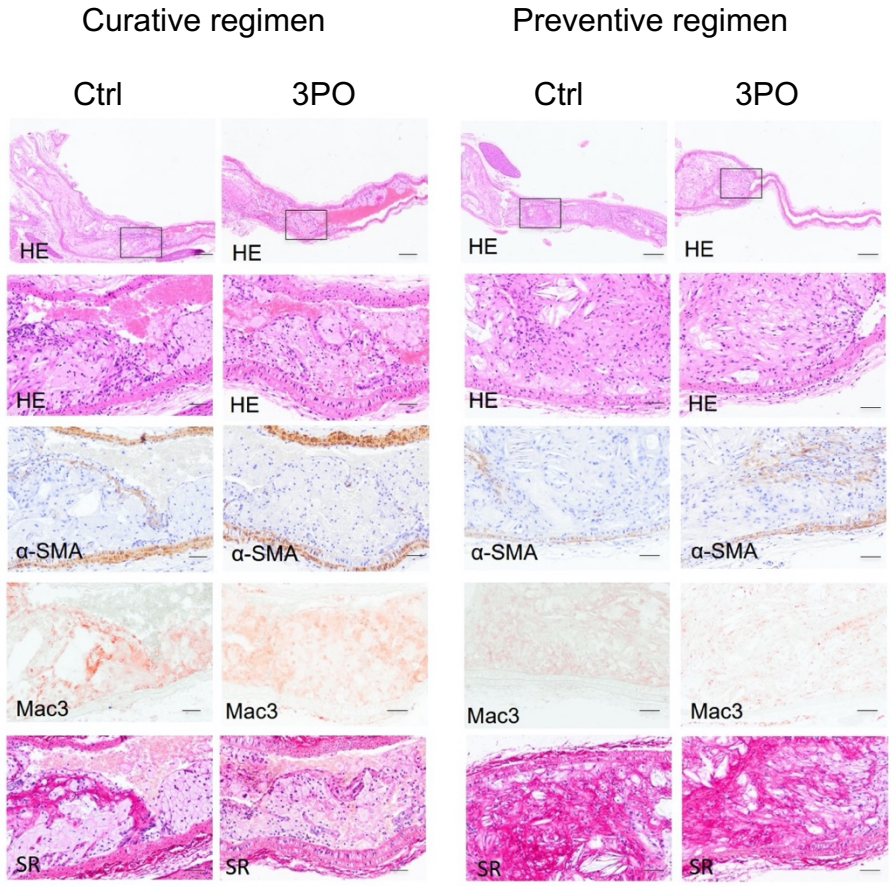

Figure IV. Histological analysis of atherosclerotic plaques in the right carotid artery of ApoE$^{-/-}$Fbn1$^{C1039G+/-}$ mice after a curative or preventive treatment regimen with 3PO. The plaque formation index and plaque thickness were measured on (HE)-stained longitudinal sections. Macrophages and smooth muscle cells were detected via immunohistochemistry using Mac-3 and α-SMC actin (α-SMA) antibodies, respectively. Collagen deposition was analysed after staining with Sirius red (SR). Representative images for each staining are shown. For quantification of the different stainings, see Table 2. Scale bar = 500 µm (first row) or 50 µm (other rows).

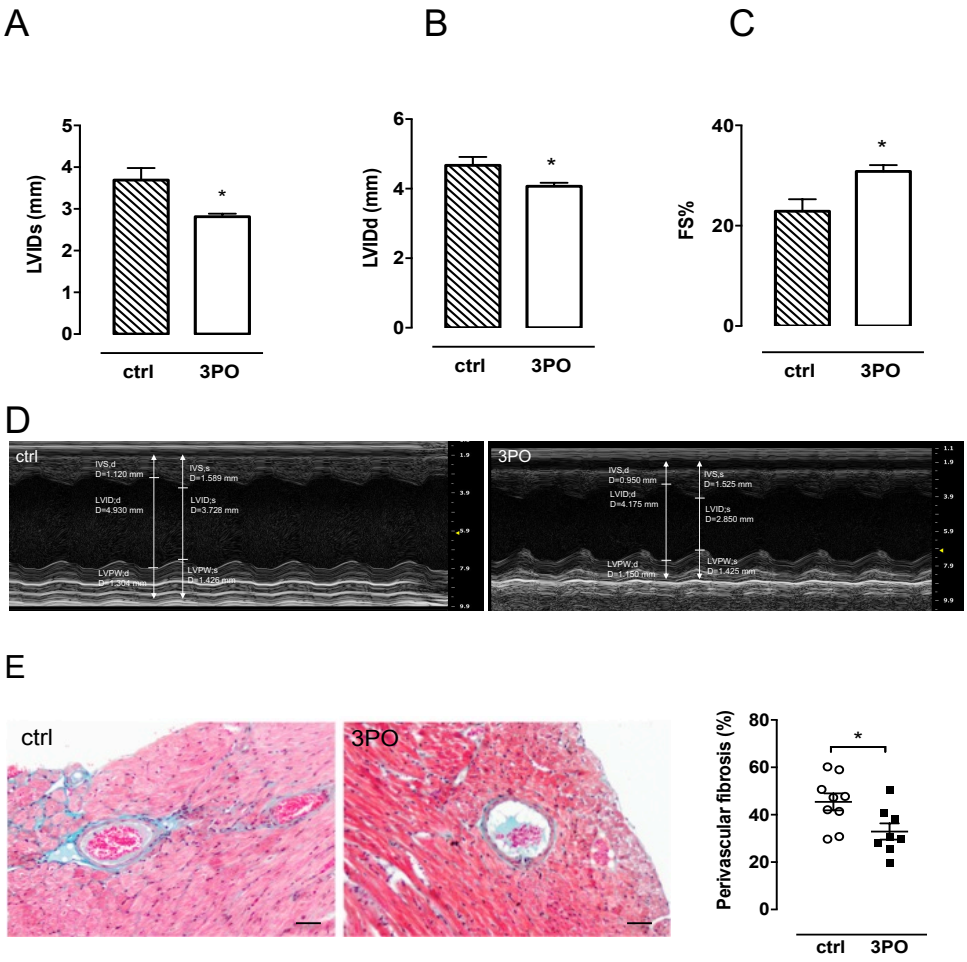

Figure V. 3PO improves the cardiac morphology and function in atherosclerotic ApoE$^{-/-}$Fbn1$^{C1039G+/-}$ mice. Measurements of left ventricular internal diameter (LVID) during systole (A) and diastole (B) in control mice versus treated mice (preventive regimen). Panel (C) represents the fractional shortening (FS) as a measure of cardiac function. **P*<0.05 (Independent samples t-test; n=12-15). (D) Representative echocardiographic images of short axis view in M-mode tracing the LV at the level of papillary muscle in control mice (left panel) and 3PO-treated mice (right panel). LVID = Left ventricle internal diameter. LVPW = Left ventricle posterior wall. IVS = interventricular septal thickness. -d = in diastole, -s = in systole. (E) Histological analysis of perivascular fibrosis around coronary arteries via Masson's trichrome staining in ApoE$^{-/-}$Fbn1$^{C1039G+/-}$ mice. Scale bar = 50 µm. **P*<0.05 (unpaired Student's t-test; control: n=9, 3PO: n=8).

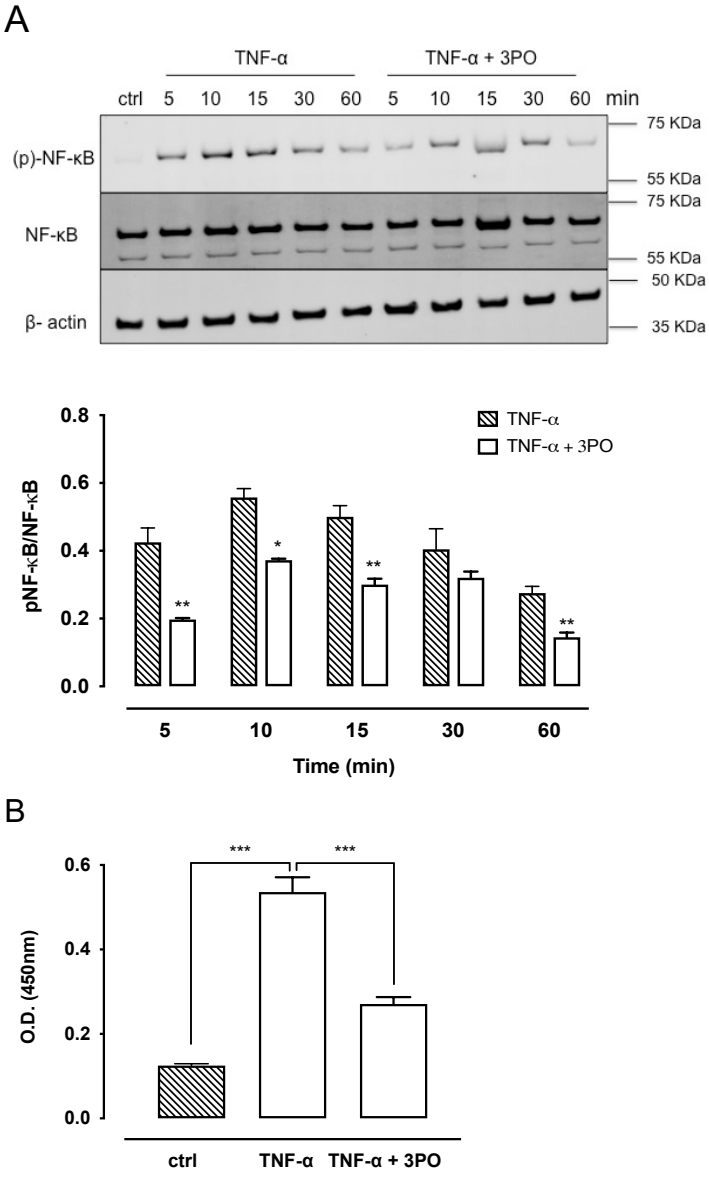

Figure VI. 3PO inhibits TNF-α-mediated NF-κB activation in endothelial cells. Human aortic endothelial cells were treated with hTNF-α (20 ng/ml) for 5, 10, 15, 30, 60 minutes in the presence or absence of 3PO (20 μM). (A) Western blot analysis of NF-κB phosphorylation (pNF-κB) and total NF-κB. Bars represent the ratio of pNF-κB over total NF-κB normalized to the loading control β-actin. **P*<0.05, ***P*<0.01 (unpaired Student's t-test; n=3). (B) DNA binding activity of NF-κB as measured by ELISA. ****P*<0.001(one-way ANOVA, followed by Bonferroni multiple comparisons test, n=3).

References

1. Carmeliet P. Angiogenesis in health and disease. *Nat Med*. 2003;9:653-660
2. Sedding DG, Boyle EC, Demandt JAF, Sluimer JC, Dutzmann J, Haverich A, Bauersachs J. Vasa vasorum angiogenesis: Key player in the initiation and progression of atherosclerosis and potential target for the treatment of cardiovascular disease. *Front Immunol*. 2018;9:706
3. Sluimer JC, Kolodgie FD, Bijnens AP, Maxfield K, Pacheco E, Kutys B, Duimel H, Frederik PM, van Hinsbergh VW, Virmani R, Daemen MJ. Thin-walled microvessels in human coronary atherosclerotic plaques show incomplete endothelial junctions relevance of compromised structural integrity for intraplaque microvascular leakage. *J Am Coll Cardiol*. 2009;53:1517-1527
4. Virmani R, Kolodgie FD, Burke AP, Finn AV, Gold HK, Tulenko TN, Wrenn SP, Narula J. Atherosclerotic plaque progression and vulnerability to rupture: Angiogenesis as a source of intraplaque hemorrhage. *Arterioscler Thromb Vasc Biol*. 2005;25:2054-2061
5. Vasudev NS, Reynolds AR. Anti-angiogenic therapy for cancer: Current progress, unresolved questions and future directions. *Angiogenesis*. 2014;17:471-494
6. Camare C, Pucelle M, Negre-Salvayre A, Salvayre R. Angiogenesis in the atherosclerotic plaque. *Redox Biol*. 2017;12:18-34
7. De Bock K, Georgiadou M, Schoors S, Kuchnio A, Wong BW, Cantelmo AR, Quaegebeur A, Ghesquiere B, Cauwenberghs S, Eelen G, Phng LK, Betz I, Tembuyser B, Brepoels K, Welti J, Geudens I, Segura I, Cruys B, Bifari F, Decimo I, Blanco R, Wyns S, Vangindertael J, Rocha S, Collins RT, Munck S, Daelemans D, Imamura H, Devlieger R, Rider M, Van Veldhoven PP, Schuit F, Bartrons R, Hofkens J, Fraisl P, Telang S, Deberardinis RJ, Schoonjans L, Vinckier S, Chesney J, Gerhardt H, Dewerchin M, Carmeliet P. Role of pfkfb3-driven glycolysis in vessel sprouting. *Cell*. 2013;154:651-663

8. Pircher A, Treps L, Bodrug N, Carmeliet P. Endothelial cell metabolism: A novel player in atherosclerosis? Basic principles and therapeutic opportunities. *Atherosclerosis*. 2016;253:247-257
9. Schoors S, De Bock K, Cantelmo AR, Georgiadou M, Ghesquiere B, Cauwenberghs S, Kuchnio A, Wong BW, Quaegebeur A, Goveia J, Bifari F, Wang X, Blanco R, Tembuyser B, Cornelissen I, Bouche A, Vinckier S, Diaz-Moralli S, Gerhardt H, Telang S, Cascante M, Chesney J, Dewerchin M, Carmeliet P. Partial and transient reduction of glycolysis by pfkfb3 blockade reduces pathological angiogenesis. *Cell Metab*. 2014;19:37-48
10. Clem B, Telang S, Clem A, Yalcin A, Meier J, Simmons A, Rasku MA, Arumugam S, Dean WL, Eaton J, Lane A, Trent JO, Chesney J. Small-molecule inhibition of 6-phosphofructo-2-kinase activity suppresses glycolytic flux and tumor growth. *Mol Cancer Ther*. 2008;7:110-120
11. Boyd S, Brookfield JL, Critchlow SE, Cumming IA, Curtis NJ, Debreczeni J, Degorce SL, Donald C, Evans NJ, Groombridge S, Hopcroft P, Jones NP, Kettle JG, Lamont S, Lewis HJ, MacFaull P, McLoughlin SB, Rigoreau LJ, Smith JM, St-Gallay S, Stock JK, Turnbull AP, Wheatley ER, Winter J, Wingfield J. Structure-based design of potent and selective inhibitors of the metabolic kinase pfkfb3. *J Med Chem*. 2015;58:3611-3625
12. Emini Veseli B, Perrotta P, De Meyer GRA, Roth L, Van der Donckt C, Martinet W, De Meyer GRY. Animal models of atherosclerosis. *Eur J Pharmacol*. 2017;816:3-13
13. Van der Donckt C, Van Herck JL, Schrijvers DM, Vanhoutte G, Verhoye M, Blockx I, Van Der Linden A, Bauters D, Lijnen HR, Sluimer JC, Roth L, Van Hove CE, Fransen P, Knaapen MW, Hervent AS, De Keulenaer GW, Bult H, Martinet W, Herman AG, De Meyer GRY. Elastin fragmentation in atherosclerotic mice leads to intraplaque neovascularization, plaque rupture, myocardial infarction, stroke, and sudden death. *Eur Heart J*. 2015;36:1049-1058
14. Van Herck JL, De Meyer GRY, Martinet W, Van Hove CE, Foubert K, Theunis MH, Apers S, Bult H, Vrints CJ, Herman AG. Impaired fibrillin-1 function promotes features of plaque instability in apolipoprotein e-deficient mice. *Circulation*. 2009;120:2478-2487

15. Chistiakov DA, Melnichenko AA, Myasoedova VA, Grechko AV, Orekhov AN. Role of lipids and intraplaque hypoxia in the formation of neovascularization in atherosclerosis. *Ann Med*. 2017;49:661-677
16. Mizushima N, Yamamoto A, Matsui M, Yoshimori T, Ohsumi Y. In vivo analysis of autophagy in response to nutrient starvation using transgenic mice expressing a fluorescent autophagosome marker. *Mol Biol Cell*. 2004;15:1101-1111
17. Daugherty A, Tall AR, Daemen M, Falk E, Fisher EA, Garcia-Cardena G, Lusis AJ, Owens AP, 3rd, Rosenfeld ME, Virmani R, American Heart Association Council on Arteriosclerosis T, Vascular B, Council on Basic Cardiovascular S. Recommendation on design, execution, and reporting of animal atherosclerosis studies: A scientific statement from the american heart association. *Arterioscler Thromb Vasc Biol*. 2017;37:e131-e157
18. Robinet P, Milewicz DM, Cassis LA, Leeper NJ, Lu HS, Smith JD. Consideration of sex differences in design and reporting of experimental arterial pathology studies-statement from atvb council. *Arterioscler Thromb Vasc Biol*. 2018;38:292-303
19. Martinet W, Timmermans JP, De Meyer GRY. Methods to assess autophagy in situ--transmission electron microscopy versus immunohistochemistry. *Methods Enzymol*. 2014;543:89-114
20. Blankenberg S, Barbaux S, Tiret L. Adhesion molecules and atherosclerosis. *Atherosclerosis*. 2003;170:191-203
21. Gimbrone MA, Jr., Garcia-Cardena G. Endothelial cell dysfunction and the pathobiology of atherosclerosis. *Circ Res*. 2016;118:620-636
22. Tawakol A, Singh P, Mojena M, Pimentel-Santillana M, Emami H, MacNabb M, Rudd JH, Narula J, Enriquez JA, Traves PG, Fernandez-Velasco M, Bartrons R, Martin-Sanz P, Fayad ZA, Tejedor A, Bosca L. Hif-1alpha and pfkfb3 mediate a tight relationship between proinflammatory activation and anerobic metabolism in atherosclerotic macrophages. *Arterioscler Thromb Vasc Biol*. 2015;35:1463-1471
23. Jablonski KA, Amici SA, Webb LM, Ruiz-Rosado Jde D, Popovich PG, Partida-Sanchez S, Guerau-de-Arellano M. Novel markers to delineate murine m1 and m2 macrophages. *PLoS One*. 2015;10:e0145342

24. Orecchioni M, Ghosheh Y, Pramod AB, Ley K. Macrophage polarization: Different gene signatures in m1(lps+) vs. Classically and m2(lps-) vs. Alternatively activated macrophages. *Front Immunol*. 2019;10:1084
25. de Vries MR, Quax PH. Plaque angiogenesis and its relation to inflammation and atherosclerotic plaque destabilization. *Curr Opin Lipidol*. 2016;27:499-506
26. Rajabi M, Mousa SA. The role of angiogenesis in cancer treatment. *Biomedicines*. 2017;5
27. Van der Veken B, De Meyer GRY, Martinet W. Intraplaque neovascularization as a novel therapeutic target in advanced atherosclerosis. *Expert Opin Ther Targets*. 2016;20:1247-1257
28. Carmeliet P. Vegf as a key mediator of angiogenesis in cancer. *Oncology*. 2005;69 Suppl 3:4-10
29. Moreo A, Vallerio P, Ricotta R, Stucchi M, Pozzi M, Musca F, Meani P, Maloberti A, Facchetti R, Di Bella S, Giganti MO, Sartore-Bianchi A, Siena S, Mancia G, Giannattasio C. Effects of cancer therapy targeting vascular endothelial growth factor receptor on central blood pressure and cardiovascular system. *Am J Hypertens*. 2016;29:158-162
30. Ali L, Schnitzler JG, Kroon J. Metabolism: The road to inflammation and atherosclerosis. *Curr Opin Lipidol*. 2018;29:474-480
31. Beldman TJ, Malinova TS, Desclos E, Grootemaat AE, Misiak ALS, van der Velden S, van Roomen C, Beckers L, van Veen HA, Krawczyk PM, Hoebe RA, Sluimer JC, Neele AE, de Winther MPJ, van der Wel NN, Lutgens E, Mulder WJM, Huveneers S, Kluza E. Nanoparticle-aided characterization of arterial endothelial architecture during atherosclerosis progression and metabolic therapy. *ACS Nano*. 2019;13:13759-13774
32. Bielenberg DR, Zetter BR. The contribution of angiogenesis to the process of metastasis. *Cancer J*. 2015;21:267-273
33. Roth L, Rombouts M, Schrijvers DM, Lemmens K, De Keulenaer GW, Martinet W, De Meyer GRY. Chronic intermittent mental stress promotes atherosclerotic plaque vulnerability, myocardial infarction and sudden death in mice. *Atherosclerosis*. 2015;242:288-294

34. Michel JB, Virmani R, Arbustini E, Pasterkamp G. Intraplaque haemorrhages as the trigger of plaque vulnerability. *Eur Heart J*. 2011;32:1977-1985, 1985a, 1985b, 1985c
35. Kolodgie FD, Gold HK, Burke AP, Fowler DR, Kruth HS, Weber DK, Farb A, Guerrero LJ, Hayase M, Kutys R, Narula J, Finn AV, Virmani R. Intraplaque hemorrhage and progression of coronary atheroma. *N Engl J Med*. 2003;349:2316-2325
36. Davies MJ, Gordon JL, Gearing AJ, Pigott R, Woolf N, Katz D, Kyriakopoulos A. The expression of the adhesion molecules icam-1, vcam-1, pecam, and e-selectin in human atherosclerosis. *J Pathol*. 1993;171:223-229
37. Cantelmo AR, Conradi LC, Brajic A, Goveia J, Kalucka J, Pircher A, Chaturvedi P, Hol J, Thienpont B, Teuwen LA, Schoors S, Boeckx B, Vriens J, Kuchnio A, Veys K, Cruys B, Finotto L, Treps L, Stav-Noraas TE, Bifari F, Stapor P, Decimo I, Kampen K, De Bock K, Haraldsen G, Schoonjans L, Rabelink T, Eelen G, Ghesquiere B, Rehman J, Lambrechts D, Malik AB, Dewerchin M, Carmeliet P. Inhibition of the glycolytic activator pfkfb3 in endothelium induces tumor vessel normalization, impairs metastasis, and improves chemotherapy. *Cancer Cell*. 2016;30:968-985
38. O'Brien KD, Allen MD, McDonald TO, Chait A, Harlan JM, Fishbein D, McCarty J, Ferguson M, Hudkins K, Benjamin CD, et al. Vascular cell adhesion molecule-1 is expressed in human coronary atherosclerotic plaques. Implications for the mode of progression of advanced coronary atherosclerosis. *J Clin Invest*. 1993;92:945-951
39. Klarer AC, O'Neal J, Imbert-Fernandez Y, Clem A, Ellis SR, Clark J, Clem B, Chesney J, Telang S. Inhibition of 6-phosphofructo-2-kinase (pfkfb3) induces autophagy as a survival mechanism. *Cancer Metab*. 2014;2:2
40. Michiels CF, Apers S, De Meyer GRY, Martinet W. Metformin attenuates expression of endothelial cell adhesion molecules and formation of atherosclerotic plaques via autophagy induction. *Annals of Clinical & Experimental Metabolism*. 2016:1(1): 1001
41. Vion AC, Kheloufi M, Hammoutene A, Poisson J, Lasselin J, Devue C, Pic I, Dupont N, Busse J, Stark K, Lafaurie-Janvore J, Barakat AI, Loyer X,

Souyri M, Viollet B, Julia P, Tedgui A, Codogno P, Boulanger CM, Rautou PE. Autophagy is required for endothelial cell alignment and atheroprotection under physiological blood flow. *Proc Natl Acad Sci U S A*. 2017;114:E8675-E8684

42. Salminen A, Kaarniranta K. Glycolysis links p53 function with nf-kappab signaling: Impact on cancer and aging process. *J Cell Physiol*. 2010;224:1-6
43. Zhang R, Li R, Liu Y, Li L, Tang Y. The glycolytic enzyme pfkfb3 controls tnf-alpha-induced endothelial proinflammatory responses. *Inflammation*. 2019;42:146-155
44. Telang S, Clem BF, Klarer AC, Clem AL, Trent JO, Bucala R, Chesney J. Small molecule inhibition of 6-phosphofructo-2-kinase suppresses t cell activation. *J Transl Med*. 2012;10:95
45. Bosca L, Gonzalez-Ramos S, Prieto P, Fernandez-Velasco M, Mojena M, Martin-Sanz P, Alemany S. Metabolic signatures linked to macrophage polarization: From glucose metabolism to oxidative phosphorylation. *Biochem Soc Trans*. 2015;43:740-744
46. McGarry T, Biniecka M, Gao W, Cluxton D, Canavan M, Wade S, Wade S, Gallagher L, Orr C, Veale DJ, Fearon U. Resolution of tlr2-induced inflammation through manipulation of metabolic pathways in rheumatoid arthritis. *Sci Rep*. 2017;7:43165
47. Khurana R, Simons M, Martin JF, Zachary IC. Role of angiogenesis in cardiovascular disease: A critical appraisal. *Circulation*. 2005;112:1813-1824
48. Dai Z, Aoki T, Fukumoto Y, Shimokawa H. Coronary perivascular fibrosis is associated with impairment of coronary blood flow in patients with non-ischemic heart failure. *J Cardiol*. 2012;60:416-421
49. Roth L, Rombouts M, Schrijvers DM, Martinet W, De Meyer GRY. Cholesterol-independent effects of atorvastatin prevent cardiovascular morbidity and mortality in a mouse model of atherosclerotic plaque rupture. *Vascul Pharmacol*. 2016;80:50-58
50. Abdellatif M, Sedej S, Carmona-Gutierrez D, Madeo F, Kroemer G. Autophagy in cardiovascular aging. *Circ Res*. 2018;123:803-824

51. Theodorou K, Boon RA. Endothelial cell metabolism in atherosclerosis. *Front Cell Dev Biol*. 2018;6:82

52. Perrotta P, Emini Veseli B, Van der Veken B, Roth L, Martinet W, De Meyer GRY. Pharmacological strategies to inhibit intraplaque angiogenesis in atherosclerosis. *Vascul Pharmacol*. 2019;112:72-78